

Digital and analog memory devices based on 2D layered MPS_3 (M=\,Mn, Co, Ni) materials

Guihua Zhao(赵贵华), Li Wang(王力), Xi Ke(柯曦), and Zhiyi Yu(虞志益)

Citation: Chin. Phys. B, 2021, 30 (**4**): 047303. DOI: 10.1088/1674-1056/abd397
Journal homepage: http://cpb.iphy.ac.cn; http://iopscience.iop.org/cpb

What follows is a list of articles you may be interested in

Recent progress on the prediction of two-dimensional materials using CALYPSO

Cheng Tang(唐程), Gurpreet Kour, Aijun Du(杜爱军)
Chin. Phys. B, 2019, 28 (**10**): 107306. DOI: 10.1088/1674-1056/ab41ea

Effects of oxygen vacancy concentration and temperature on memristive behavior of $SrRuO_3$/Nb:$SrTiO_3$ junctions

Zhi-Cheng Wang(王志成), Zhang-Zhang Cui(崔璋璋), Hui Xu(徐珲), Xiao-Fang Zhai(翟晓芳), Ya-Lin Lu(陆亚林)
Chin. Phys. B, 2019, 28 (**8**): 087303. DOI: 10.1088/1674-1056/28/8/087303

Electronic and magnetic properties of CrI_3 nanoribbons and nanotubes

Ji-Zhang Wang(王吉章), Jian-Qi Huang(黄建啟), Ya-Ning Wang(王雅宁), Teng Yang(杨腾), Zhi-Dong Zhang(张志东)
Chin. Phys. B, 2019, 28 (**7**): 077301. DOI: 10.1088/1674-1056/28/7/077301

Electronic synapses based on ultrathin quasi-two-dimensional gallium oxide memristor

Shuopei Wang(王硕培), Congli He(何聪丽), Jian Tang(汤建), Rong Yang(杨蓉), Dongxia Shi(时东霞), Guangyu Zhang(张广宇)
Chin. Phys. B, 2019, 28 (**1**): 017304. DOI: 10.1088/1674-1056/28/1/017304

Room-temperature infrared photodetectors with hybrid structure based on two-dimensional materials

Tiande Liu(刘天德), Lei Tong(童磊), Xinyu Huang(黄鑫宇), Lei Ye(叶镭)
Chin. Phys. B, 2019, 28 (**1**): 017302. DOI: 10.1088/1674-1056/28/1/017302

Digital and analog memory devices based on 2D layered MPS$_3$ (M = Mn, Co, Ni) materials*

Guihua Zhao(赵贵华)[1], Li Wang(王力)[4], Xi Ke(柯曦)[3,†], and Zhiyi Yu(虞志益)[1,2,‡]

[1] School of Electronics and Information Technology, Sun Yat-sen University, Guangzhou 510006, China
[2] School of Microelectronics Science and Technology, Sun Yat-sen University, Zhuhai 519082, China
[3] School of Materials and Energy, Guangdong University of Technology, Guangzhou 510006, China
[4] School of Chemistry and Chemical Engineering, Neijiang Normal University, Neijiang 641100, China

(Received 4 October 2020; revised manuscript received 18 November 2020; accepted manuscript online 15 December 2020)

We demonstrate digital and analog devices with an Ag/MPS$_3$/Au structure based on layered MPS$_3$ (M = Mn, Co, Ni) 2D materials. All devices show the bipolar behavior of resistive switching. In addition, Ag/MnPS$_3$/Au and Ag/NiPS$_3$/Au devices show synaptic characteristics of potentiation and depression. The digital and analog characteristics of resistance states enable Ag/MPS$_3$/Au devices to work as both binary memory and artificial synapse devices. The Ag/MPS$_3$/Au memory devices are promising for applications of flexible eye-like and brain-like systems on a chip when they are integrated with photodetectors and FETs composed of full MPS$_3$ materials.

Keywords: electrochemical metallization memory, memristor, 2D materials, neuromorphic computing

PACS: 73.61.–r, 68.37.–d, 68.55.ag **DOI:** 10.1088/1674-1056/abd397

1. Introduction

Memristors as an electronic synapse is promising in applications of the next-generation artificial neural network, which has attracted extensive research interest.[1–8] According to the mechanisms, the memristors can be mainly classified into three categories: valence change memories (VCM), thermochemical memories (TCM) and electrochemical metallization memories (ECM).[9,10] ECM-based device consists of a thin film of solid electrolyte sandwiched between two electrodes, one is an active metal layer (Ag or Cu) and the other is an inert metal layer (Au or Pt).[11] The solid electrolyte layer acts as an ionic conductor where the active metal ions can migrate under the electrical field.[12] The conductive filament (CF) of active metal is deposited and dissolved between the electrodes with electrical stimulations, which is associated with redox reaction.[11] This process results in resistive switching (RS) for devices. When the CF bridges the electrodes, a device can enter a low resistance state (LRS), otherwise it is in a high resistance state (HRS). Due to dual resistance states, devices were widely used as binary storages. On the other hand, multiple resistance states make devices promising as an artificial synapse suitable for neuromorphic computing.[13]

A vertical structure is popularly used for ECM-based devices because it occupies less space than a planar structure and can be stacked three dimensionally.[14] Memristors based on 2D materials have many advantages such as low-power consumption and high-frequency operation and temperature tolerance.[15–17] The 2D materials such as transition metal dichalcogenide (TMD), hexagonal boron nitride (h-BN) and MXene have been used as electrolytes in ECM-based devices.[9,18,19] However, memory devices based on three-element 2D materials are seldom reported. Some layered MPS$_3$ (M = transition metal) materials have ionic conductivity and their single crystals can be exfoliated to a few atomic layers.[20–22] In addition, MPS$_3$ compounds are semiconductors or insulators with wide band gaps of 1.3–3.5 eV, which can support large ON/OFF resistance ratios for ECM-based devices.[20] Moreover, the ultra-violet (UV) photodetectors, FETs and ECM-based devices composed of full MPS$_3$ 2D materials may be integrated to perform the combined functions of perception, storage and computing in a system on a chip (SOC).[18,23,24] This SOC is suitable for applications of flexible and intelligent vision systems for UV light images with low latency and low-power consumption. Therefore, it is essential to explore ECM-based devices using layered MPS$_3$ materials.

Recently, we reported a memristor based on a layered FePS$_3$ 2D material.[25] This device shows dual modes of resistive switching with digital and analog features, which makes the device suitable for complex neuromorphic system. It implies the potential of 2D MPS$_3$ materials working as electrolyte in ECM-based devices. In addition, UV photodetector and FETs of 2D MPS$_3$ materials have been widely reported.[26–29] However, the memory devices based on 2D MPS$_3$ (M = Mn, Co, Ni) materials have not been reported. This limits the exploration and application of eye-like and

*Project supported by the National Key R&D Program of China (Grant Nos. 2017YFA0206200 and 2018YFB2202601) and the National Natural Science Foundation of China (Grant Nos. 61674173, 61834005, and 61902443).

†Corresponding author. E-mail: kexi@gdut.edu.cn
‡Corresponding author. E-mail: yuzhiyi@mail.sysu.edu.cn

© 2021 Chinese Physical Society and IOP Publishing Ltd

brain-like systems based on MPS$_3$ 2D materials. Therefore, it needs further exploration to obtain more knowledge and enrich the diversity which can increase possibility of potential applications for these devices.

In this work, vertical devices with a structure of Ag/MPS$_3$/Au (M = Mn, Co, Ni) are introduced. The bipolar RS behavior with sweep voltages are demonstrated. The synaptic potentiation and depression with both sweep and pulse voltages are shown. The results indicate Ag/MPS$_3$/Au devices are promising as both binary memory and synaptic devices.

2. Experimental detail

2.1. Crystal synthesis

MPS$_3$ (M = Mn, Co, Ni) single crystals were grown by the same chemical vapor transport (CVT) method as reported in Ref. [25]. First, high-purity powders of M, P, S and I_2 were mixed according to the mole ratio of 1:1:3:0.0293. The total mass of M, P and S is 1151.37 mg. Then, the mixed powder was transferred to the bottom of a quartz tube in a glove box filled with inert atmosphere. Next, the quartz tube was sealed under the atmospheric pressure of 0.1 Pa with oxyhydrogen flame. Finally, the tube was put in a two-temperature zone furnace and heated slowly to the target temperatures, 690 °C (hot zone) and 620 °C (cold zone) which keep for two weeks. Then, the single crystals were obtained.

2.2. Device fabrication

The Ag/MPS$_3$/Au (M = Mn, Co, Ni) cross-point devices were fabricated on a silicon oxide substrate. The fabrication procedure consists of three major steps: definition of a bottom electrode, transfer of an MPS$_3$ layer and definition of a top electrode. Both metal layers were obtained by lift-off after patterning and the overlap between the electrodes defines the switch region. The Au/Ti bottom electrode with an enlarged pad was created with a width of 4–5 μm and a thickness of 100/10 nm. Next, an MPS$_3$ flake was transferred onto the bottom electrode by polydimethylsiloxane (PDMS) after mechanical exfoliation with Scotch tape under an optical microscope.[30] Lastly, the top Ag electrode with a width of 12–13 μm and a thickness of 120 nm was created using the same fabrication process as bottom electrode. All the patterning was operated by laser direct writing (LDW) photolithography on an exposure machine of uPG501 which has enough precision (0.5 μm) for this work and lower cost than electron beam lithography (EBL). All the coating was implemented by electron beam evaporation in a DE400 system.

2.3. Sample characterization

The thicknesses of the MPS$_3$ layers of the devices were measured by an atomic force microscope (AFM, NT-MDT NTEGRA Spectra). The electrical measurements of a sweep mode were investigated by a source-meter (KEYSIFHT B2912A), and the synaptic measurements by pulse stimulations were performed by the combination the source-meter (KEYSIFHT B2912A) and a control system (ENlitech RM15001). The elements of MPS$_3$ crystals were observed by an energy dispersive spectrometer (EDS) together with a scanning electron microscope (SEM, HITACHI SU8010).

3. Results and discussion

Layered MPS$_3$ (M = Mn, Co, Ni) single crystals have a monoclinic structure with space group $C2/m$.[20] MPS$_3$ layers of hexagonal lattices are weakly bonded together through van der Waals interactions (Fig. 1(a)). It is obvious that the as-synthesized MPS$_3$ (the nominal atom ratio 1:1:3 is used in the whole paper) single crystals have layered structures and are highly crystalline shown in SEM images (Figs. 1(b)–1(c), Figs. S1–S3).

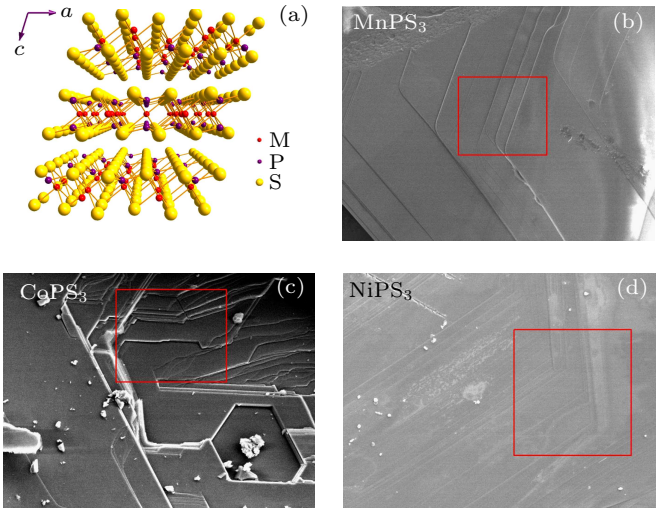


Fig. 1. The structure and morphology of as-grown single crystals of MPS$_3$ (M = Mn, Co, Ni), the red rectangles indicate the regions for EDS observation.

Vertical Ag/MPS$_3$/Au (M = Mn, Co, Ni) devices were fabricated by the methods described above. As shown in Fig. 2(a), an MPS$_3$ single-crystalline layer is sandwiched between the Ag top electrode and the Au bottom electrode. The device forms a structure of crossbar where Ag and Au layers show white and yellow colors respectively. The overlap between electrodes define the switch areas, where 2D material layers have single colors with uniform thicknesses (Figs. 2(b)–2(d)). The thicknesses of MnPS$_3$, CoPS$_3$, NiPS$_3$ layers are approximately 82 nm (126 layers), 93 nm (146 layers) and 114 nm (180 layers), respectively (Figs. S4–S6). The layer number is equal to the thickness of a 2D material divided by the interlayer spacing (see details in Table S1). The crossbar areas are 4×12 μm^2, 4×12 μm^2 and 5×13 μm^2 for Ag/MnPS$_3$/Au, Ag/CoPS$_3$/Au and Ag/NiPS$_3$/Au devices, respectively.

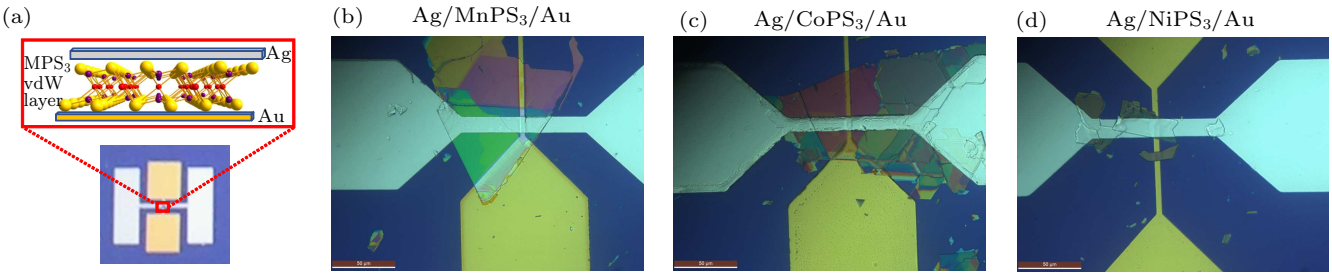


Fig. 2. The structure and morphology of Ag/MPS$_3$/Au (M = Mn, Co, Ni) devices.

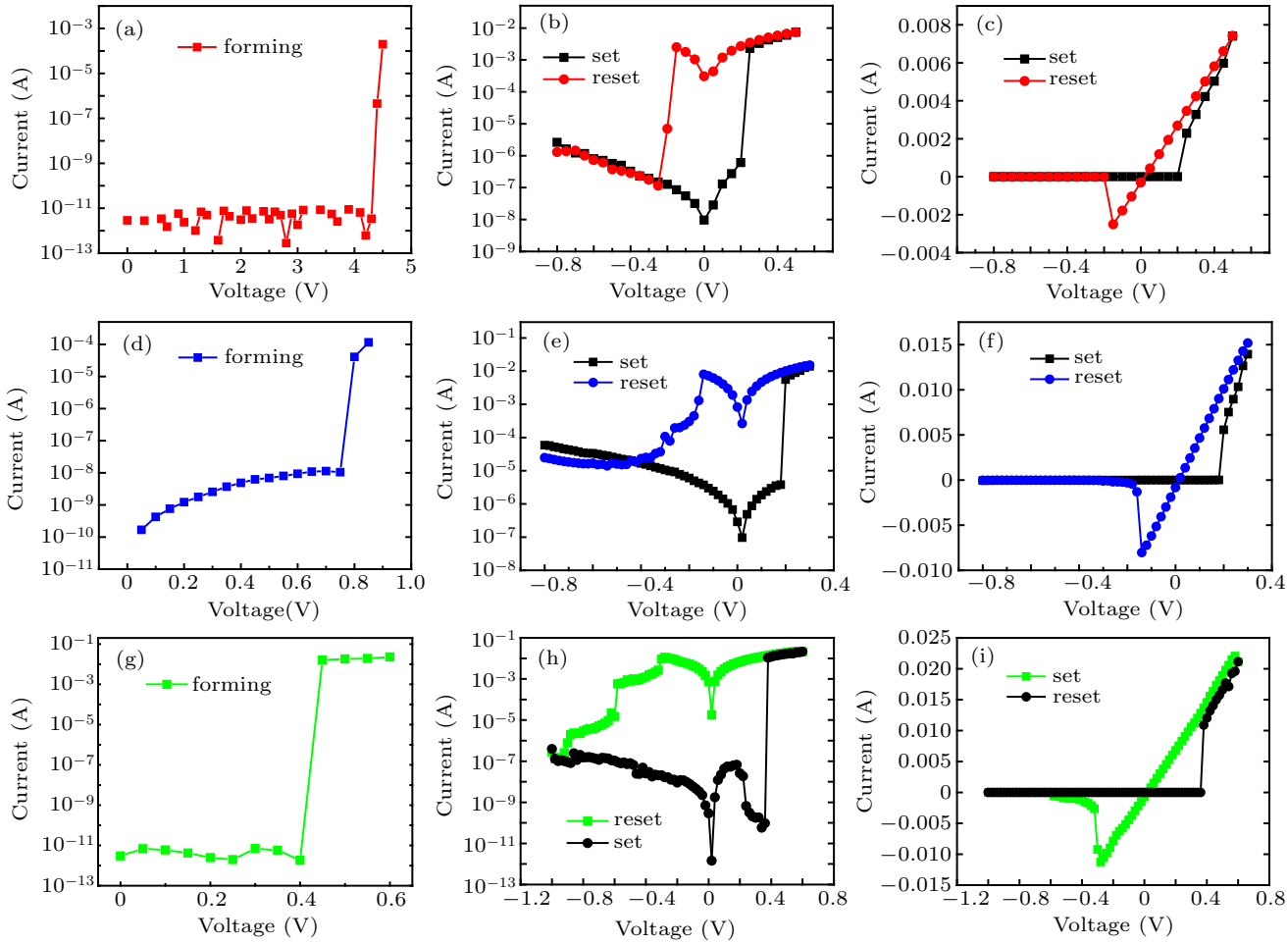


Fig. 3. The forming processes and the bipolar behaviors of resistive switching for Ag/MPS$_3$/Au (M = Mn, Co, Ni) devices. [(a), (b), (c)] Corresponding to an Ag/MnPS$_3$/Au device. [(d), (e), (f)] Corresponding to an Ag/CoPS$_3$/Au device. [(g), (h), (i)] Corresponding to an Ag/NiPS$_3$/Au device. [(c), (f), (i)] Linear expressions corresponding to [(b), (e), (h)].

The current-voltage (I–V) curves exhibit behaviors of bipolar RS. Initially, the currents are less than 10^{-9} A at an HRS. Then, the currents jump to over 10^{-4} A and reaches an LRS after the sweep voltages reach the threshold values of 4.25 V, 0.75 V and 0.4 V with a compliance current of 0.1 A (Figs. 3(a), 3(d), 3(g)). After these forming processes, the bipolar RS occurs with applications of positive and negative sweep voltages. When the positive voltages are higher than the thresholds ($V_{\rm set}$), the resistance changes from HRS to LRS. On the contrary, the negative voltages turn the resistance from LRS to HRS at the thresholds ($V_{\rm reset}$) (Figs. 3(b), 3(c), 3(e), 3(f), 3(h), 3(i)). The ON/OFF resistance ratios reach 10^3, which enables Ag/MPS$_3$/Au devices to be taken as binary memories with high readability. The linear expressions of I–V curves show Ohm behaviors, which implies formation of Ag conductive bridges in the MPS$_3$ layers. Moreover, the bipolar characteristics are consistent with the reported Ag$_2$S-based switch, FePS$_3$ and CrPS$_4$-based synaptic devices.[25,31–33] Therefore, the RS may be attributed to formation and rupture of Ag conductive bridges, which originate from the Ag ion migration and redox reaction.[11,25,33] It should be noted that the reset processes include more than two RS steps for Ag/CoPS$_3$/Au and Ag/NiPS$_3$/Au devices, which implies the possibility of multi-level RS to be discussed thereinafter. For the Ag/MnPS$_3$/Au and Ag/CoPS$_3$/Au devices, the switching voltages are close to 0.2 V, which is compara-

ble with Cu/MoS_2 double-layer/Au device that has the lowest switching voltages among 2D materials-based memristors.[34] In addition, the few-layer UV photodetectors based on $MnPS_3$ and $NiPS_3$ have been reported. The integration of photodetectors and binary memory composed of full 2D materials will enable the device suitable for a flexible and wearable eye-like system in a chip (SOC) with perception and memory functions.[23]

Besides digital RS, Ag/MPS$_3$/Au (M = Mn, Ni) devices also manifest analogue RS behaviors like artificial synapses. For an Ag/$NiPS_3$/Au device, DC sweep voltages were applied to measure the potentiation and depression. When consecutive positive (0 to 0.2 V) and negative (0 to −0.2 V) sweep voltages were applied, its currents gradually increase and decrease, respectively (Figs. 4(a) and 4(b)). This result implies existence of multiple resistance states which can be achieved by sweep voltages. The similar behaviors were also reported for synaptic devices based on MoS_2, $FePS_3$, $CrPS_4$ and Ag_2S.[25,32–34] The conductance is at the level of 100 Ω, which means that Ag CFs keep electrodes connected. This analogue RS behavior may be attributed to modulation of overall cross-sectional areas of CFs.[32,34] It is similar for an Ag/$MnPS_3$/Au device. With consecutive application of positive and negative pulse voltages (an amplitude of 0.2 V, a duration of 10 ms, an interval of 50 ms), the resistance decreases and increases between 150 Ω and 5000 Ω, respectively (Figs. 4(c) and 4(d)). The Ag/$MnPS_3$/Au device also shows multiple resistance states achievable by pulse voltages. The resistance of the Ag atomic contact (12.9 kΩ) was defined as the threshold of the ON state, according to which the Ag/$MnPS_3$/Au device remains in the ON state with the application of pulse voltages.[32] The resistance was not set back to the initial HRS with the negative pulse voltages. This implies existence of other conductive paths which are not ruptured. The integration of synaptic devices and FETs composed of full MPS$_3$ 2D materials is suitable for a flexible brain-like SOC.[18]

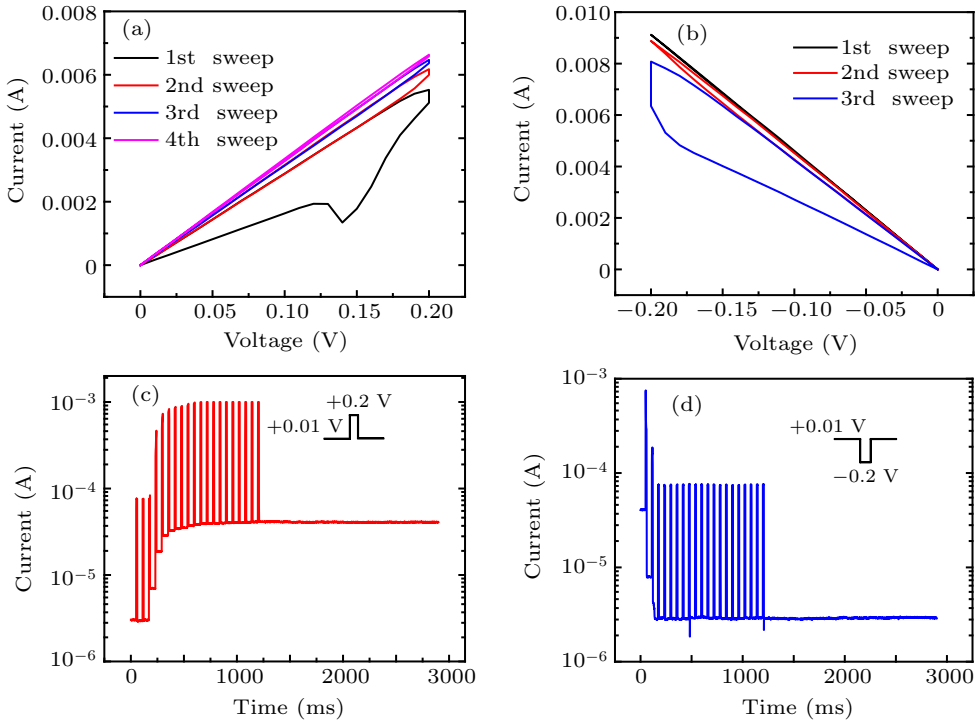


Fig. 4. The behaviors of potentiation and depression for Ag/MPS$_3$/Au devices. [(a), (b)] Corresponding to an Ag/$NiPS_3$/Au device with positive and negative sweep voltages between 0 and +0.2 V/−0.2 V. [(c), (d)] Corresponding to an Ag/$MnPS_3$/Au device with positive and negative pulse voltages respectively (amplitude = 0.2 V, duration = 10 ms, interval = 50 ms). The read voltage during the intervals is 0.01 V.

4. Conclusions

In summary, we have demonstrated digital and analogue memory devices with an Ag/MPS$_3$/Au structure based on layered MPS$_3$ (M = Mn, Co, Ni) 2D materials. All the devices show bipolar RS behavior. Ag/$MnPS_3$/Au and Ag/$NiPS_3$/Au devices show synaptic characteristics of potentiation and depression. The digital and analog characteristics enable the Ag/MPS$_3$/Au devices suitable for the flexible eye-like and brain-like systems on a chip, especially when they are integrated with photodetectors and FETs composed of full MPS$_3$ materials.

Acknowledgement

The authors acknowledge the support by Dr. Yiyan Wang from Institute of Physics, CAS.

References

[1] Pershin Y V and Di Ventra M 2011 *Adv. Phys.* **60** 145
[2] Kuzum D, Yu S and Wong H S 2013 *Nanotechnology* **24** 382001
[3] Shao N, Zhang S B and Shao S Y 2019 *Acta Phys. Sin.* **68** 198502 (in Chinese)

[4] Liu Y C, Lin Y, Wang Z Q and Xu H Y 2019 *Acta Phys. Sin.* **68** 168504 (in Chinese)

[5] Xue W H, Ci W J, Xu X H and Liu G 2020 *Chin. Phys. B* **29** 48401

[6] Yang B B, Xu N, Zhou E R, Li Z W, Li C, Yi P Y and Fang L 2020 *Chin. Phys. B* **29** 48505

[7] Xu W, Wang Y Q, Li Y F, Gao F, Zhang M C, Lian X J, Wan X, Xiao J and Tong Y 2019 *Acta Phys. Sin.* **68** 238501 (in Chinese)

[8] Liu H J, Chen C L, Zhu X, Sun S Y, Li Q J and Li Z W 2020 *Chin. Phys. B* **29** 28502

[9] Zhang L, Gong T, Wang H, Guo Z and Zhang H 2019 *Nanoscale* **11** 12413

[10] Yang R 2020 *Chin. Phys. B* **29** 097305

[11] Waser R, Dittmann R, Staikov G and Szot K 2009 *Adv. Mater.* **21** 2632

[12] Shi S Q, Gao J, Liu Y, Zhao Y, Wu Q, Ju W W, Ouyang C Y and Xiao R J 2016 *Chin. Phys. B* **25** 018212

[13] Hasegawa T, Terabe K, Tsuruoka T and Aono M 2012 *Adv. Mater.* **24** 252

[14] Shi Y Y, Liang X H, Yuan B, Chen V, Li H T, Hui F, Yu Z C W, Yuan F, Pop E, Wong H S P and Lanza M 2018 *Nat. Electron.* **1** 458

[15] Zhao H, Dong Z P, Tian H, DiMarzi D, Han M G, Zhang L H, Yan X D, Liu F X, Shen L, Han S J, Cronin S, Wu W, Tice J, Guo J and Wang H 2017 *Adv. Mater.* **29** 1703232

[16] Kim M, Ge R J, Wu X H, Lan X, Tice J, Lee J C and Akinwande D 2018 *Nat. Commun.* **9** 2524

[17] Wang M, Cai S H, Pan C, Wang C Y, Lian X J, Zhuo Y, Xu K, Cao T J, Pan X Q, Wang B G, Liang S J, Yang J J, Wang P and Miao F 2018 *Nat. Electron.* **1** 130

[18] Wang C Y, Wang C, Meng F H, Wang P F, Wang S, Liang S J and Miao F 2019 *Adv. Electron. Mater.* **6** 1901107

[19] Chen Y H, Xu W, Wang Y Q, Wan X, Li Yue F, Liang D K, Lu L Q, Liu X W, Lian X J, Hu E T, Guo Y F, Xu J G, Tong Y and Xiao J 2019 *Acta Phys. Sin.* **68** 098501 (in Chinese)

[20] Susner M A, Chyasnavichyus M, McGuire M A, Ganesh P and Maksymovych P 2017 *Adv. Mater.* **29** 1602852

[21] Long G, Henck H, Gibertini M, Dumcenco D, Wang Z, Taniguchi T, Watanabe K, Giannini E and Morpurgo A F 2020 *Nano Lett.* **20** 2452

[22] Lee J U, Lee S, Ryoo J H, Kang S, Kim T Y, Kim P, Park C H, Park J G and Cheong H 2016 *Nano Lett.* **16** 7433

[23] Chen S, Lou Z, Chen D and Shen G Z 2018 *Adv. Mater.* **30** 1705400

[24] Wang S, Wang C, Wang P, Wang C, Li Z, Pan Dai Y, Gao A, Liu C, Liu J, Yang H, Liu X, Cheng, B, Chen K, Wang Z, Watanabe K, Taniguchi T, Liang S and Miao F 2020 *Natl. Sci. Rev.* **8** nwaa172

[25] Zhao G, Ke X, Li X, Wang L, Yin N, Jin X, Chen J, Xu Yi, Wang K, Yu X, Yu Z 2020 *Appl. Phys. Express* **13** 105001

[26] Kumar R, Jenjeti R N, Austeria M P and Sampath S 2019 *J. Mater. Chem. C* **7** 324

[27] Gao Y, Lei S J, Kang T T, Fei L F, Mak C L, Yuan J, Zhang M G, Li S J, Bao Q L, ZengZ M, Wang Z, Gu H S and Zhang K 2018 *Nanotechnology* **29** 244001

[28] Chu J W, Wang F M, Yin L, Lei L, Yan C Y, Wang F, Wen Y, Wang Z X, Jiang C, Feng L P, Xiong J, Li Y R and He J 2017 *Adv. Funct. Mater.* **27** 1701342

[29] Jenjeti R N, Kumar R, Austeria M P and Sampath S 2018 *Sci. Rep.* **8** 8586

[30] Zhang X W, He D W, He J Q, Zhao S Q, Hao S C, Wang Y S and Yi L X 2017 *Chin. Phys. B* **26** 097202

[31] Hino T, Tanaka H, Hasegawa T, Aono M and Ogawa T 2010 *Small* **6** 1745

[32] Hasegawa T, Ohno T, Terabe K, Tsuruoka T, Nakayama T, Gimzewski J K and Aono M 2010 *Adv. Mater.* **22** 1831

[33] Lee M J, Lee S, Lee S, Balamurugan K, Yoon C, Jang J T, Kim S H, Kwon D H, Kim M, Ahn J P, Kim D H, Park J G and Park B H 2018 *NPG Asia Mater.* **10** 23

[34] Xu R, Jang H, Lee M H, Amanov D, Cho Y, Kim H, Park S, Shin H J and Ham D 2019 *Nano Lett.* **19** 2411